eISSN 2747-1381

Vol 00 no 0x (202x), pages 000-000

Jurnal Mekanik Terapan

(Journal of Applied Mechanics)

Available on: http://jurnal.pnj.ac.id/index.php/jmt

Analysis of the Effect of Sootblowers on Superheater Heat Transfer Rates in Units 2 and 3 of the Indramayu Steam Power Plant (PLTU)

Ardi Wibowo[1], Paulus Sukusno[1*], dan Candra Damis Widiawaty[1]

[1]Program Studi Teknologi Rekayasa Pembangkit Energi, Department of Mechanical Engineering, Politeknik Negeri Jakarta, Jl. Prof. G. A. Siwabessy, Kampus UI, Depok, 16425

*Corresponding author: paulus.sukusno@mesin.pnj.ac.id

Article info: Received: dd Month yyyy | Accepted: dd Month yyyy | Available online: dd Month yyyy

DOI: 10.32722/jmt.vXiX.xxxx

Abstract

Coal ash fouling on boiler superheater tubes causes a reduction in power plant thermal efficiency. This study analyzes the effect of sootblower operation on the heat transfer rate (Q) of Unit 2 and Unit 3 superheaters at Indramayu Power Plant. Secondary data from the Distributed Control System (DCS) were collected for 9 hours before and 9 hours after sootblowing under stable load conditions. The value of Q was calculated using $Q = \dot{m}(hout - hin)$ with enthalpy values from IAPWS-IF97 steam tables. Results show that average Q for Unit 2 increased from 83.24 MW to 89.80 MW (a 7.88% rise) with a 7.37°C increase in outlet steam temperature. For Unit 3, average Q increased from 80.27 MW to 89.93 MW (a 12.03% rise) with a 10.98°C temperature increase. For the single sootblowing cycle observed in each unit, sootblower operation was associated with a clear increase in superheater heat transfer rate, indicating its potential as a reference for evaluating boiler cleaning schedules.

Keywords: sootblower, fouling, superheater, heat transfer rate, PLTU Indramayu

1. INTRODUCTION

Electric power is a fundamental need that underpins nearly every sector of modern life. In Indonesia, electricity demand continues to rise in line with economic and population growth. According to PLN Statistics 2023, the total installed capacity of PLN Group power plants reached 45,095.19 MW, with coal-fired steam power plants (PLTU) as the largest contributor at 20,439.90 MW, or around 28% of the total [1]. When captive power plants are also taken into account, the operating capacity of coal-fired power plants in 2024 reached approximately 51.56 GW [2]. This heavy reliance of the national electricity system on coal-fired power plants means that their operational reliability and efficiency have a direct bearing on national energy security.

The most critical component of a coal-fired power plant is the boiler, which converts the chemical energy of coal combustion into thermal energy in the form of high-pressure steam. Inside the boiler, the superheater heats saturated steam into superheated steam before it is delivered to the turbine. The quality of the steam leaving the superheater, reflected in its temperature and pressure, largely determines both turbine efficiency and the overall thermal performance of the plant [3]. Maintaining heat transfer performance in the superheater is therefore one of the main priorities in power plant operation.

However, coal combustion continuously produces fly ash and mineral deposits that adhere to the outer surface of the superheater tubes. The accumulation of these deposits is known as fouling, which acts as a thermal insulator that increases thermal resistance, lowers the heat transfer rate, raises flue gas exit temperature, and reduces overall boiler efficiency [4]. Sandberg et al. [5] demonstrated, through a dynamic simulation of a biomass-fired circulating fluidized bed boiler, that ash deposits accumulating on heat transfer surfaces substantially increase thermal resistance and progressively degrade heat transfer performance as the deposit layer thickens, an effect that is particularly significant for plants in the hundreds-of-megawatt range. Quantitatively, the impact of fouling can be expressed through the fouling factor (R_f), which represents the additional thermal resistance introduced by the deposit layer [6]. A comparable degradation pattern has also been reported on other convective heating surfaces such as reheaters, where the buildup of fouling resistance directly dictates how frequently a heating surface needs to be cleaned [7].

To address fouling, PLTU boilers are equipped with sootblowers that periodically spray high-pressure steam onto the tube surfaces to dislodge deposits without interrupting boiler operation [4]. Tong et al. [8] showed that every sootblowing event on a 300 MW coal-fired boiler significantly and consistently reduced the thermal resistance of the ash layer, directly indicating a recovery of heat transfer rate. Madejski and Taler [9] showed that sootblower activation produces rapid and measurable changes in tube wall temperature that can be tracked through operational parameters, while Taler et al. [10] confirmed that the presence of ash deposits affects both the tube wall temperature distribution and overall heat transfer performance. Granda et al. [11] obtained a flue-gas-side heat transfer coefficient of 159.96–189.63 W/(m²·K) under full-load conditions, a value that can serve as a plausibility benchmark for calculation results. More recently, Xu et al. [12] specifically analyzed a platen superheater in a coal-fired power plant boiler and confirmed, through a heat-loss-based analysis, that soot blowing measurably restores heat transfer performance that had been degraded by ash deposition on this type of heating surface.

Even so, most of the recent literature on sootblower and fouling performance has been dominated by model-based, optimization, or machine-learning approaches developed and validated mainly on boilers outside Indonesia, for example soot-blowing optimization models for air preheaters and economizers [13], ash fouling prediction using hybrid neural network methods [14], optimal soot-blowing control based on the Hamilton-Jacobi-Bellman equation [15], CFD-artificial neural network based soot-blowing optimization [16], and reinforcement-learning-based optimization of ash deposit removal [17]. Studies that specifically analyze the effect of sootblower operation on superheater heat transfer rate in Indonesian coal-fired power plants using actual operational data remain relatively limited, as most prior work is either simulation-based or relies on data from boilers abroad. Indramayu Power Plant, owned by PT PLN Nusantara Power, has three units with a capacity of 330 MW each. At the time this study was conducted, Unit 1 was undergoing an overhaul while Unit 2 and Unit 3 were operating actively, allowing direct observation and data collection on both units. Even among operational-data studies such as Xu et al. [12], which analyzed a single platen superheater in one boiler using a heat-loss-based method, the novelty of the present study lies in evaluating the sootblower effect on two boilers of identical design operating in parallel at the same plant, using a direct enthalpy-based heat transfer rate calculation validated against the IAPWS-IF97 Region 2 formulation. This paired-unit design allows the consistency of the sootblower effect to be checked across two nominally identical boilers, which is not addressed in prior single-unit operational studies. This study aims to calculate the superheater heat transfer rate of Unit 2 and Unit 3 before and after sootblower operation, and to analyze its effect on the increase in heat transfer rate in each unit based on actual operational data.

2. RESEARCH METHOD

2.1. Research Type and Object

This study uses a quantitative descriptive approach. The quantitative approach was chosen because the main variable, the heat transfer rate (Q), is numerical and can be calculated directly from pressure, temperature, and steam flow rate data, making the result objective and reproducible. The descriptive nature of the study is intended to describe the effect of sootblower operation on Q for the object under observation, without any experimental manipulation.

The object of this study is the sootblower and superheater system of Unit 2 and Unit 3 at Indramayu Power Plant, located at Jl. Pramuka No. 01, Sukra, Indramayu Regency, West Java. The superheater was selected as the object of analysis because it is the final steam-heating stage before the turbine, is located in a high-temperature flue gas path that makes it more prone to fouling, and has complete and continuous inlet and outlet parameters available in the DCS. Analysis was carried out separately for each unit to determine the consistency of the sootblower effect on two boilers with identical design specifications, rather than to compare which unit performs better.

2.2. Data Source and Sampling Method

The data used are quantitative secondary data sourced from the Distributed Control System (DCS) of Unit 2 and Unit 3. The DCS continuously records operational parameters directly from instrumentation installed on the superheater piping (pressure, temperature, and flow transmitters), so that it represents actual operating conditions without disrupting production, while also enabling data extraction for specific time windows before and after a given sootblowing event. The parameters required for this study are shown in Table 1.

Table 1. Data parameters used in this study

No.	Parameter
1	Superheater inlet steam pressure, Pin (bar)
2	Superheater inlet steam temperature, Tin (°C)
3	Superheater outlet steam pressure, Pout (bar)
4	Superheater outlet steam temperature, Tout (°C)
5	Superheater steam flow rate (kg/hour)
6	Unit operating load (MW)
7	Sootblower operating time and duration

Sampling was carried out by selecting one representative sootblower operating cycle for each unit, namely a cycle that occurred under relatively stable operating load conditions. A stable load condition (change of less than 1%) is important to ensure that the observed change in Q purely reflects the effect of the sootblower rather than load fluctuation acting as a confounding factor. Data were collected for a window of 9 hours before and 9 hours after sootblowing, with a recording interval of 1 hour (9 data points per condition), so that the trend of parameter change could be observed progressively. The operating load conditions at the time of sampling are shown in Table 2.

For Unit 2, the sootblowing cycle observed began at 16:00 and was completed by 17:30, so the before-sootblowing window covers 08:00–16:00 and the after-sootblowing window covers 17:30–01:30. For Unit 3, sootblowing began at 18:00 and was completed by 20:15, giving a before-sootblowing window of 10:00–18:00 and an after-sootblowing window of 20:15–04:15. All pressure, temperature, and flow readings were taken from the permanently installed DCS transmitters at the superheater inlet and outlet headers, the same instruments used for routine plant monitoring, so no additional sensors were installed for this study. One representative cycle per unit was analyzed because only one sootblowing event during the observation period met the stable-load criterion (load change below 1%) without being confounded by other simultaneous operational changes (e.g., load ramping, other maintenance activity); additional cycles recorded during the data collection period were excluded for this reason. The 9-hour window before and after sootblowing was chosen to be long enough to capture the outlet steam temperature trend before it re-stabilizes after cleaning while remaining within a period of consistently stable load, matching the operational shift pattern at the plant. Other operational variables that could influence the heat transfer rate but were not directly controlled for in this study, such as flue gas exit temperature, coal feed rate, excess air ratio, and attemperator spray-water flow, were not part of the parameter set extracted from the DCS for this analysis and are addressed as a limitation in Section 3.5.

Table 2. Unit operating load conditions at the time of sampling

Unit	Average load before SB (MW)	Average load after SB (MW)	Remarks
Unit 2	300.2	300.1	Relatively stable load
Unit 3	300.1	300.0	Relatively stable load

2.3. Data Analysis Method

The heat transfer rate absorbed by the superheater was calculated using the specific steam enthalpy difference between the outlet and inlet sides, as expressed in Equation (1) [6].

$$Q = \dot{m} \times (h_{out} - h_{in}) \qquad (1)$$

eISSN 2747-1381

Jurnal Mekanik Terapan (Journal of Applied Mechanics) vol 00 no 0x (202x), pages 000-000

where Q is the heat transfer rate (kW), ṁ is the steam mass flow rate (kg/s), and h_{out} and h_{in} are the specific enthalpy of the outlet and inlet superheater steam (kJ/kg), respectively. The enthalpy-based equation was chosen because enthalpy is a state function that directly reflects the total energy of the steam. The alternative approach $Q = \dot{m} \times c_p \times \Delta T$ assumes a constant specific heat (c_p), whereas for high-pressure superheated steam (around 160–175 bar, as in the Indramayu Power Plant superheater) the value of c_p changes significantly with pressure and temperature, so that using a constant c_p has the potential to introduce a considerable error [18].

Specific steam enthalpy values were determined based on the standard IAPWS-IF97 steam tables [19]. Because the pressure and temperature values recorded by the DCS generally fall between the grid points of the table, two-dimensional linear interpolation was used, namely interpolation with respect to temperature on two reference pressure rows followed by interpolation with respect to pressure, as expressed in Equation (2).

$$h(x) = h_0 + [(h_1 - h_0) / (x_1 - x_0)] \times (x - x_0) \qquad (2)$$

where h(x) is the specific enthalpy being sought, h_0 and h_1 are the specific enthalpies at the reference conditions x_0 and x_1 (pressure or temperature). Validation against one data point showed that the difference between the linear interpolation result and a direct calculation using the IAPWS-IF97 Region 2 formulation was below 0.01%, so that this method was considered accurate and defensible. The resulting Q values and outlet steam temperature trends are presented in tables and charts so that the change in trend can be analyzed visually and effectively.

3. RESULTS AND DISCUSSION

3.1. Data Collection and Processing

Secondary data from the DCS in the form of pressure (bar), temperature (°C), and steam flow rate (kg/hour) on the inlet and outlet sides of the superheater were grouped into two samples based on the unit observed (Unit 2 and Unit 3) and analyzed separately. At each time point, the inlet-side enthalpy (h_{in}) and outlet-side enthalpy (h_{out}) were calculated using two-dimensional linear interpolation on the IAPWS-IF97 steam tables. As an illustration of the method, one data point from Unit 2 at 08:00 (before sootblowing) is presented in Table 3, with the corresponding pressure and temperature conditions.

Table 3. Example of operational data on the inlet and outlet sides of the superheater (Unit 2, 08:00)

Side	Pressure (bar)	Temperature (°C)
Inlet	171.71	439.40
Outlet	166.06	532.66

For P_{out} = 166.06 bar and T_{out} = 532.66°C, applying Equation (2) to the nearest grid points (P = 165 and 170 bar; T = 530 and 535°C) gives h_{out} = 3384.52 kJ/kg, and the same two-step interpolation gives h_{in} = 3079.00 kJ/kg, so Δh = 305.52 kJ/kg. The same procedure was applied to every data point for both units using Microsoft Excel, and the results are summarized in Tables 4 through 7.

3.2. Effect of Sootblower on Unit 2 Heat Transfer Rate

Table 4. Calculated enthalpy and heat transfer rate of Unit 2 (before sootblowing)

Time	hin (kJ/kg)	hout (kJ/kg)	Δh (kJ/kg)	ṁ (kg/s)	Q (MW)
08:00	3,079.04	3,384.53	305.49	272.028	83.102
09:00	3,084.93	3,392.17	307.24	273.283	83.965
10:00	3,084.34	3,385.51	301.17	272.351	82.023
11:00	3,080.24	3,391.23	311.00	272.546	84.761
12:00	3,080.99	3,391.99	310.99	272.944	84.883
13:00	3,084.55	3,390.59	306.04	272.659	83.444
14:00	3,088.67	3,388.78	300.11	273.297	82.020

Time	hin (kJ/kg)	hout (kJ/kg)	Δh (kJ/kg)	ṁ (kg/s)	Q (MW)
15:00	3,090.40	3,392.42	302.03	271.046	81.863
16:00	3,085.03	3,392.05	307.03	270.754	83.128

Table 5. Calculated enthalpy and heat transfer rate of Unit 2 (after sootblowing)

Time	hin (kJ/kg)	hout (kJ/kg)	Δh (kJ/kg)	ṁ (kg/s)	Q (MW)
17:30	3,076.80	3,417.89	341.09	267.290	91.171
18:30	3,076.29	3,414.16	337.87	267.162	90.266
19:30	3,077.44	3,411.27	333.83	267.312	89.237
20:30	3,077.97	3,413.70	335.73	268.442	90.123
21:30	3,083.53	3,415.60	332.08	265.819	88.272
22:30	3,079.66	3,414.56	334.91	266.030	89.096
23:30	3,078.73	3,413.48	334.75	266.788	89.307
00:30	3,074.31	3,413.68	339.36	267.192	90.675
01:30	3,080.67	3,415.09	334.42	269.178	90.020

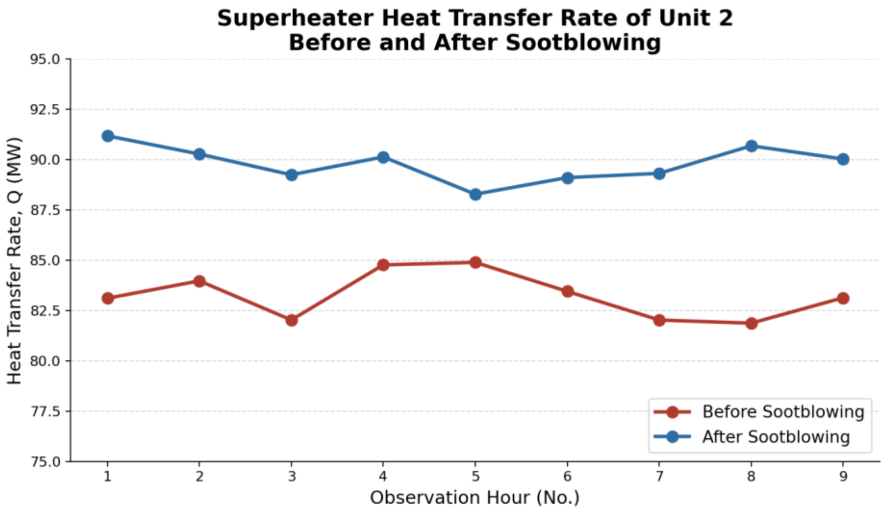

Figure 1. Heat transfer rate before and after sootblowing on Unit 2

Tables 4 and 5 present the calculated enthalpy and heat transfer rate of the Unit 2 superheater before and after sootblowing. The average Q increased from 83.24 MW to 89.80 MW. Figure 1 shows that Q after sootblowing was consistently higher than Q before sootblowing at every observation point, with the highest Q after cleaning reaching 91.17 MW compared with only 84.88 MW beforehand. This increase indicates that the sootblower successfully reduced the fouling layer, lowering thermal resistance and making heat transfer from the flue gas to the steam more efficient, consistent with the principle that ash deposits act as a thermal insulator [4].

3.3. Effect of Sootblower on Unit 3 Heat Transfer Rate

Table 6. Calculated enthalpy and heat transfer rate of Unit 3 (before sootblowing)

Time	hin (kJ/kg)	hout (kJ/kg)	Δh (kJ/kg)	ṁ (kg/s)	Q (MW)
10:00	3,088.49	3,387.35	298.86	267.515	79.950
11:00	3,083.13	3,384.90	301.76	268.140	80.914
12:00	3,089.88	3,387.92	298.03	268.662	80.070

Time	hin (kJ/kg)	hout (kJ/kg)	Δh (kJ/kg)	ṁ (kg/s)	Q (MW)
13:00	3,092.34	3,391.65	299.31	269.323	80.611
14:00	3,095.83	3,389.23	293.40	267.718	78.548
15:00	3,091.16	3,391.23	300.07	269.740	80.941
16:00	3,092.60	3,390.08	297.47	268.713	79.935
17:00	3,093.03	3,397.28	304.26	267.988	81.537
18:00	3,096.18	3,394.34	298.15	268.260	79.983

Table 7. Calculated enthalpy and heat transfer rate of Unit 3 (after sootblowing)

Time	hin (kJ/kg)	hout (kJ/kg)	Δh (kJ/kg)	ṁ (kg/s)	Q (MW)
20:15	3,079.17	3,427.80	348.63	264.104	92.075
21:15	3,083.05	3,424.91	341.86	264.520	90.429
22:15	3,080.55	3,423.68	343.13	261.435	89.707
23:15	3,087.52	3,429.11	341.59	264.001	90.180
00:15	3,084.24	3,424.10	339.86	262.717	89.286
01:15	3,085.61	3,424.81	339.20	264.765	89.808
02:15	3,085.13	3,422.07	336.94	264.014	88.958
03:15	3,085.25	3,426.46	341.21	262.584	89.595
04:15	3,084.51	3,423.93	339.42	263.227	89.345

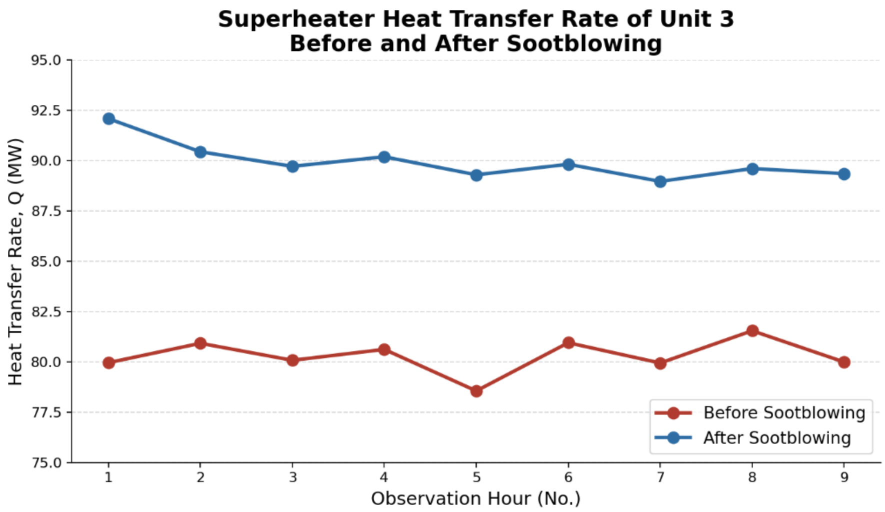

Figure 2. Heat transfer rate before and after sootblowing on Unit 3

The calculation results for the Unit 3 superheater are shown in Tables 6 and 7. The average Q increased from 80.27 MW to 89.93 MW. A pattern similar to Unit 2 is also observed for Unit 3 (Figure 2), namely that Q after sootblowing was consistently higher than Q before sootblowing at every time point, with the highest Q reaching 92.08 MW compared with only 81.54 MW before cleaning. This again shows that sootblower operation successfully restored the condition of the superheater tube surface from fouling.

eISSN 2747-1381

Jurnal Mekanik Terapan (Journal of Applied Mechanics) vol 00 no 0x (202x), pages 000-000

3.4. Summary and Discussion

In both units, outlet steam temperature increased after the sootblower was operated: for Unit 2, from an average of 533.98°C to 541.35°C (an increase of 7.37°C), and for Unit 3, from an average of 533.16°C to 544.14°C (an increase of 10.98°C). This increase in T_{out} is consistent with the increase in Q, since more efficient heat transfer produces steam with a higher outlet temperature. A summary of the sootblower effect on both units is presented in Table 8.

Table 8. Summary of heat transfer rate and outlet steam temperature for Unit 2 and Unit 3

Parameter	Unit 2	Unit 3
Average Q before SB (MW)	83.24	80.27
Average Q after SB (MW)	89.80	89.93
Absolute ΔQ (MW)	6.56	9.66
ΔQ (%)	7.88%	12.03%
Average Tout before SB (°C)	533.98	533.16
Average Tout after SB (°C)	541.35	544.14
ΔTout (°C)	7.37	10.98
Average flow before SB (kg/hour)	980,362.93	966,423.42
Average flow after SB (kg/hour)	962,085.50	948,546.09

Based on Table 8, both units show a consistent pattern of sootblower effect, namely an increase in Q and T_{out} after the sootblower is operated, accompanied by a slight decrease in steam flow because part of the steam is consumed as the sootblower spray medium. For Unit 2, Q increased by 7.88% (6.56 MW) with a T_{out} increase of 7.37°C, while for Unit 3, Q increased by 12.03% (9.66 MW) with a T_{out} increase of 10.98°C. These two results independently demonstrate that sootblower operation has a positive effect on restoring the heat transfer rate of the superheater, consistent with the principle that removing the fouling layer lowers thermal resistance on the tube surface [4, 8]. This finding is also in line with Xu et al. [12], who found that soot blowing measurably restores the heat transfer performance of a platen superheater degraded by ash deposition, reinforcing the conclusion that the enthalpy-based Q measured in this study genuinely reflects a recovery of heat transfer capability rather than a measurement artifact.

To assess whether the observed increase in Q reflects more than ordinary hour-to-hour variability, the nine hourly Q values before and after sootblowing were compared for each unit. For Unit 2, the mean Q rose from 83.24 MW (SD = 1.14 MW) to 89.80 MW (SD = 0.89 MW); for Unit 3, from 80.28 MW (SD = 0.86 MW) to 89.93 MW (SD = 0.92 MW). An independent-samples t-test (Welch's correction, unequal variances) shows the before-after difference is statistically significant for both units (Unit 2: $t = 13.53$, $p < 0.001$; Unit 3: $t = 23.01$, $p < 0.001$), and the effect size is very large in both cases (Cohen's $d = 6.4$ for Unit 2 and 10.9 for Unit 3). The magnitude of these differences relative to the natural spread of the data supports the interpretation that sootblowing, rather than random fluctuation within each observation window, is the dominant driver of the increase in Q. This statistical result does not by itself rule out the influence of other operational variables that changed over the same time window, which is addressed further below.

The interpretation above should nonetheless be made cautiously. Because only one sootblowing cycle was observed per unit and other operational variables such as flue gas exit temperature, coal feed rate, excess air ratio, and attemperator spray-water flow were not tracked alongside Q in this study, part of the observed increase cannot be fully separated from possible concurrent changes in these variables, even though the load itself was confirmed stable. This limitation is common to before-after field studies of this type, and a similar caveat applies to comparable operational-data studies such as Tong et al. [8] and Xu et al. [12], which likewise rely on a limited number of observed cycles rather than a fully controlled experiment. The Q increase and its statistical significance are therefore best read as strong evidence of an association between sootblowing and heat transfer recovery for the conditions observed, rather than as a fully isolated causal effect.

The difference in the magnitude of the percentage increase in Q between Unit 2 and Unit 3 may be influenced by various operational factors that differ between the units, such as maintenance history, previous sootblowing schedules, or internal boiler conditions. However, further analysis of the factors causing this difference is beyond the scope of this study, which focuses on the effect of the sootblower on heat transfer rate in each unit independently, rather than on evaluating the relative effectiveness between units.

4. CONCLUSION

Based on the results and discussion, sootblower operation is shown to have a positive effect on increasing the heat transfer rate of the superheater in the Unit 2 and Unit 3 boilers at Indramayu Power Plant. For Unit 2, the average heat transfer rate increased from 83.24 MW to 89.80 MW (an increase of 6.56 MW, or 7.88%), accompanied by an average outlet steam temperature increase of 7.37°C. For Unit 3, the average heat transfer rate increased from 80.27 MW to 89.93 MW (an increase of 9.66 MW, or 12.03%), accompanied by an average outlet steam temperature increase of 10.98°C. Both units show a consistent pattern: for the single sootblowing cycle observed in each unit, sootblower operation is associated with a marked increase in superheater heat transfer rate following a period of decline attributed to fouling, although the magnitude of the increase differs between units and the study cannot fully rule out the influence of other operational factors that were not tracked. This finding underscores the importance of routine evaluation of sootblower effects based on actual operational data for each unit. Should this association be confirmed across a larger number of cycles, condition-based sootblowing strategies could be explored as a potential future application to improve cleaning effectiveness while conserving the use of high-pressure steam.

ACKNOWLEDGMENTS

The authors would like to thank PT PLN Nusantara Power UP Indramayu, particularly the Operational Planning and Control Division and the Mechanical Maintenance and Instrumentation & Control Maintenance teams, for their support with operational data and field guidance that greatly assisted the completion of this study.

REFERENCES

[1] PT PLN (Persero). Statistik PLN 2023. Jakarta: PT PLN (Persero); 2024.

[2] Wiatros-Motyka M, Fulghum N, Jones D, Altieri K, Black R, Broadbent H, et al. Global Electricity Review 2024. London: Ember; 2024.

[3] Dr. P K Nag. Power Plant Engineering. 3rd ed. New Delhi: 2005.

[4] The Babcock & Wilcox Company. Steam, its generation and use. 41st ed. Babcock & Wilcox; 2005.

[5] Sandberg J, Fdhila RB, Dahlquist E, Avelin A. Dynamic simulation of fouling in a circulating fluidized biomass-fired boiler. Appl Energy 2011;88:1813–24. https://doi.org/10.1016/j.apenergy.2010.12.006.

[6] Bergman TL, Lavine AS. Fundamentals of Heat and Mass Transfer. 8th ed. 2017.

[7] Anitha Kumari S, Srinivasan S. Ash fouling monitoring and soot-blow optimization for reheater in thermal power plant. Appl Therm Eng 2019;149:62–72. https://doi.org/10.1016/j.applthermaleng.2018.12.031.

[8] Tong S, Zhang X, Tong Z, Wu Y, Tang N, Zhong W. Online ash fouling prediction for boiler heating surfaces based on wavelet analysis and support vector regression. Energies (Basel) 2019;13. https://doi.org/10.3390/en13010059.

[9] Madejski P, Taler D. Analysis of temperature and stress distribution of superheater tubes after attemperation or sootblower activation. Energy Convers Manag 2013;71:131–7. https://doi.org/10.1016/j.enconman.2013.03.025.

[10] Taler D, Trojan M, Dzierwa P, Kaczmarski K, Taler J. Numerical simulation of convective superheaters in steam boilers. International Journal of Thermal Sciences 2018;129:320–33. https://doi.org/10.1016/j.ijthermalsci.2018.03.005.

[11] Granda M, Trojan M, Taler D. CFD analysis of steam superheater operation in steady and transient state. Energy 2020;199. https://doi.org/10.1016/j.energy.2020.117423.

[12] Xu L, Huang Y, Yue J, Chen B, Yu M, Zhu Z, et al. Soot blowing optimization for platen superheater of coal-fired power plant boiler based on heat loss analysis. Asia-Pacific Journal of Chemical Engineering 2022;17. https://doi.org/10.1002/apj.2764.

[13] Shi Y, Wen J, Cui F, Wang J. An optimization study on soot-blowing of air preheaters in coal-fired power plant boilers. Energies (Basel) 2019;12. https://doi.org/10.3390/en12050958.

[14] Shi Y, Li M, Wen J, Yang Y, Cui F, Zeng J. Heat transfer efficiency prediction of coal-fired power plant boiler based on ceemdan-nar considering ash fouling. Energies (Basel) 2021;14. https://doi.org/10.3390/en14134000.

[15] Wen J, Shi Y, Pang X, Jia J, Zeng J. Optimization of Boiler Soot Blowing Based on Hamilton-Jacobi-Bellman Equation. IEEE Access 2019;7:20850–62. https://doi.org/10.1109/ACCESS.2019.2897362.

[16] Sundaram T, Basim Ismail F, Gunnasegaran P, Gurusingam P. Development and implementation of Intelligent Soot Blowing Optimization System for TNB Janamanjung. MATEC Web of Conferences, vol. 131, EDP Sciences; 2017. https://doi.org/10.1051/matecconf/201713101006.

[17] Lim J, Cho H, Kwon H, Park H, Kim J. Reinforcement learning-based optimal operation of ash deposit removal system to improve recycling efficiency of biomass for CO2 reduction. J Clean Prod 2022;370. https://doi.org/10.1016/j.jclepro.2022.133605.

[18] Yunus AC, Michael AB. Thermodynamics An Engineering Approach. 8th ed. McGraw-Hill Education; 2015.

[19] Wagner W, Cooper JR, Dittmann A, Kijima J, Kretzschmar H-J, Kruse A, et al. The IAPWS Industrial Formulation 1997 for the Thermodynamic Properties of Water and Steam. J Eng Gas Turbines Power. 2000;122(1):150-84. https://doi.org/10.1115/1.483186.